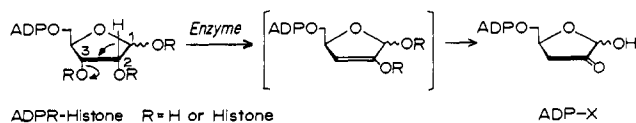
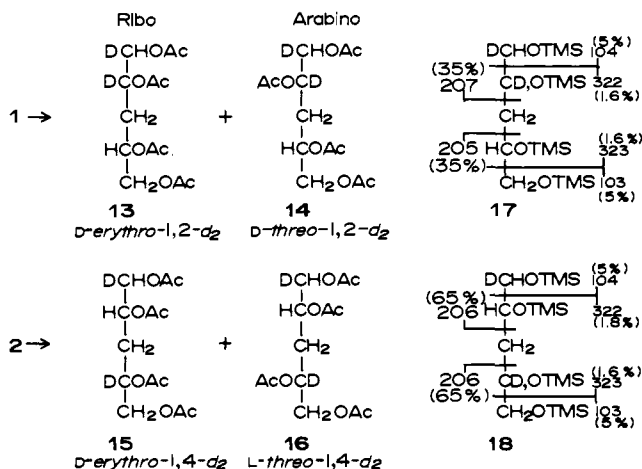


Scheme III



synthesized respectively from D-ribonolactone and D-glucose (via 7¹⁹), as shown in Schemes I and II.²⁰

The synthetic ulose and natural X were reduced with NaBD₄ in D₂O¹³ and acetylated to give pentitols-*d*₂ 13/14 and 15/16 and



the ribo and arabino forms of reduced X-*d*₂ acetates. The retention times in the GC-MS²¹ of 13/15²² (7.4 min) and 14/16²² (7.2 min) were identical with those of reduced X-*d*₂, while the MS patterns of all compounds were indistinguishable. The acetates 13-16 and reduced X-*d*₂ acetates were therefore deacetylated and trimethylsilylated²³ in situ to per-Me₃Si derivatives, which were then subjected to GC-MS²¹ to locate the D atoms in reduced X-*d*₂. Ribo and arabino isomers appeared at *t*_R 7.8 and 8.3 min, respectively, with diagnostic fragments 205/207 (17) and 206 (18). The MS fragmentation pattern of reduced X-*d*₂ Me₃Si derivatives was identical with that of 17 (Figure 1). A *D*-glycero configuration can be assigned to C-4 in X since this chiral center is the *D*-ribose C-4 in the original (ADP-ribosyl)histone. Sugar X is thus 3-deoxy-*D*-glycero-pentos-2-ulose or its hydrate.

The mechanism of sugar X formation is unclear at this stage. Although an ester linkage between the terminal ribose and glutamate residue was suggested^{2,3} for the enzyme substrate, the site

(16) These two structures have been proposed previously for some products in a complex reaction mixture obtained by γ -ray radiolysis of D-ribose: Von Sonntag, C.; Dizdaroglu, M. *Carbohydr. Res.* 1977, 58, 21.

(17) Only one anomer was detected: ¹H NMR (D₂O, 360 MHz) 4.13 (br s, 1-H), 4.01 (dddd, *J*_{4,5'} = 4.0, *J*_{4,5} = 6.8, *J*_{3,4} = 8.6, *J*_{3,4'} = 3.8 Hz, 4-H), 3.63 (dd, *J*_{5,5'} = 11.7 Hz, 5-H), 3.51 (dd, 5'-H), 2.01 (dd, *J*_{3,3'} = 14.5 Hz, 3-H), 1.95 (dd, 3'-H); CD (0.03% in D₂O) $\Delta\epsilon_{213}$ = +0.013, $\Delta\epsilon_{260}$ = -0.005, $\Delta\epsilon_{277}$ = +0.004, $\Delta\epsilon_{310}$ = -0.003; UV (0.03% in H₂O) λ_{max} 269 nm (ϵ 75).

(18) A 1:2:1 mixture of 2a, 2b, and 2c was obtained after deblocking: ¹H NMR (D₂O, 360 MHz) (2a) 4.91 (d, *J*_{1,2} = 4.9 Hz, 1-H), 4.42 (d, *J*_{5,5'} = 19.2 Hz, 5-H), 4.38 (d, 5'-H), 4.38 (d, 5'-H), 4.01 (ddd, *J*_{2,3(a)}} = 8.0, *J*_{2,3(e)}} = 4.2 Hz, 2-H), 2.74 (dd, *J*_{3,3'} = 16.4 Hz, 3(e)-H), 2.68 (dd, 3(a)-H) (2b) 4.63 (d, *J*_{1,2} = 6.7 Hz, 1-H), 3.70 (dd, *J*_{3(e),5(e)}} = 2.98 *J*_{5,5'} = 11.6 Hz, 5(e)-H), 3.62 (ddd, *J*_{2,3(a)}} = 10.5, *J*_{2,3(e)}} = 4.7 Hz, 2-H), 3.54 (d, 5(a)-H), 2.28 (ddd, *J*_{3,3'} = 13.0 Hz, 3(e)-H), 1.80 (dd, 3(a)-H) (2c) 5.12 (d, *J*_{1,2} = 3.2 Hz, 1-H), 3.92 (ddd, *J*_{2,3(a)}} = 10.6, *J*_{2,3(e)}} = 4.6 Hz, 2-H), 3.79 (d, *J*_{5,5'} = 11.7 Hz, 5(a)-H), 3.41 (dd, *J*_{3(e),5(e)}} = 2.4 Hz, 5(e)-H), 2.08 (ddd, *J*_{3,3'} = 12.8 Hz, 3(e)-H), 1.97 (dd, 3(a)-H); CD (0.2% in H₂O) $\Delta\epsilon_{265}$ = -0.017, $\Delta\epsilon_{300}$ (sh) = -0.005; UV (0.2% in H₂O) λ_{max} 270 nm (sh, ϵ 20). The ratio of 2a/2b/2c is ca. 0.5:2:1 from ¹H NMR in D₂O at the same concentration.

(19) Whistler, R. L.; Doner, L. W. *Methods Carbohydr. Chem.* 1972, 6, 215.

(20) ¹H NMR were taken for all synthetic intermediates (cf. supplementary material).

(21) OV-1 Glass-packed column, 1 m \times 0.6 cm OD, 64 mL/min He, oven temperature 100-170 $^{\circ}$ C, linear temperature gradient 4 $^{\circ}$ C/min (for acetates) or 2 $^{\circ}$ C/min (for TMS derivatives).

(22) Authentic 3-deoxypentitols were separately synthesized in order to distinguish ribo and arabino isomers.

(23) Sweeley, C. C.; Bentley, R.; Makita, M.; Wells, W. W. *J. Am. Chem. Soc.* 1963, 85, 2497.

of linkage in the ribose moiety is still unknown. However, elucidation of sugar X shows that the 3-hydroxy or 3-glutamyl group in (ADP-ribosyl)histone is eliminated by the enzyme to yield ADP-X (Scheme III).¹⁰

Acknowledgment. We are grateful to Drs. M. Hirama and J. Pawlak, SUNBOR, for valuable discussions on syntheses and MS, respectively.

Supplementary Material Available: ¹H NMR data of all synthetic intermediates, observed and simulated ¹H NMR spectra for reduced X-*d*₂ acetates, and synthesis of deoxypentitols (8 pages). Ordering information is given on any current masthead page.

Hydrogen-Bond Stabilization of Oxygen in Hemoprotein Models

Joël Mispelter,* Michel Momenteau, Daniel Lavalette, and Jean-Marc Lhoste

Unité INSERM 219, Institut Curie, Section de Biologie
Bât. 112, Centre Universitaire, 91405 ORSAY, France

Received March 7, 1983

Chemically synthesized compounds¹⁻³ permit the analysis of the relationship⁴ of the stereochemical features to the kinetic and thermodynamic properties of the oxygenated hemes. The bent structure of the dioxygen molecule relative to the symmetry axis of the hemes proposed early by Pauling⁵ is now demonstrated for oxymyoglobin⁶ and oxyhemoglobin.⁷ The stabilization of this conformation by hydrogen bond with the distal histidine residue⁵ is however still questionable, at least for its energetic contribution. Such a bond has been recently observed in sperm-whale oxymyoglobin by neutron diffraction⁸ and is likely to occur in human oxyhemoglobin, at least in the α subunits.⁷ The bent oxygen structure has been also observed in model compounds.⁹⁻¹¹ The NMR investigation of new compounds including amide groups in the vicinity of the oxygen binding site³ is now reported. It indicates a direct interaction of these groups with the oxygen molecule consistent with hydrogen-bond formation. This bond adds a free energy contribution for oxygen binding that makes the affinity of the model compounds comparable to that of the natural oxygen carriers.

The models are built up from 5,10,15,20-tetraphenylporphyrin. They include two chains bridged between opposite meso phenyl groups over both faces of the porphyrin ring. A pyridine molecule is inserted within one of these chains and acts as the proximal base. It is coordinated on the central iron(II) atom. The chain bridged over the distal face of the heme protects it from the irreversible oxidation of the oxygen complex into μ -oxo dimers.

(1) Traylor, T. G.; Traylor, P. S. *Annu. Rev. Biophys. Bioeng.* 1982, 11, 105-127.

(2) Momenteau, M.; Mispelter, J.; Loock, B.; Bisagni, E. *J. Chem. Soc., Perkin Trans. 1* 1983, 189-196.

(3) Momenteau, M.; Lavalette, D. *J. Chem. Soc., Chem. Comm.* 1982, 341-343.

(4) Perutz, M. F. *Annu. Rev. Biochem.* 1979, 48, 327-386.

(5) Pauling, L. *Nature (London)* 1964, 203, 182-183.

(6) Phillips, S. E. V. *J. Mol. Biol.* 1980, 142, 531-554.

(7) Shaanan, B. *Nature (London)* 1982, 296, 683-684.

(8) Phillips, S. E. V.; Schoenborn, B. P. *Nature (London)* 1981, 292, 81-82.

(9) Collman, J. P.; Gagne, R. R.; Reed, C. A.; Robinson, W. T.; Rodley, G. A. *Proc. Natl. Acad. Sci. U.S.A.* 1974, 71, 1326-1329.

(10) Jameson, G. B.; Rodley, G. A.; Robinson, W. T.; Gagne, R. R.; Reed, C. A.; Collman, J. P. *Inorg. Chem.* 1977, 17, 850-857.

(11) Jameson, G. B.; Molinaro, F. S.; Ibers, J. A.; Collman, J. P.; Brauman, S. I.; Rose, E.; Suslick, K. S. *J. Am. Chem. Soc.* 1980, 102, 3224-3237.

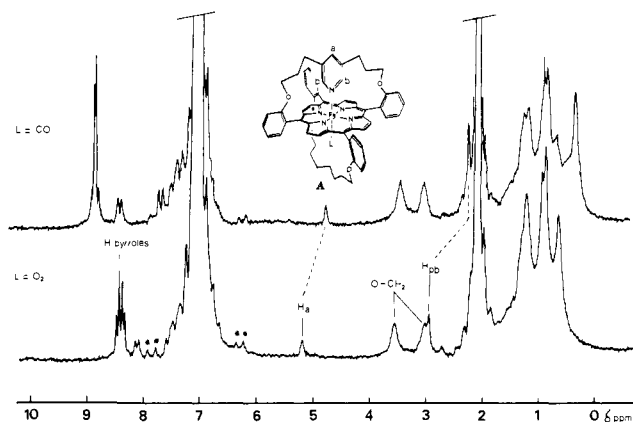


Figure 1. Proton NMR spectra of the oxygen and carbon monoxide complexes of compound A in deuterated toluene (from CEA, France) solution at 0 °C. The peaks marked by an asterisk correspond to the ^{13}C satellites of nondeuterated solvent impurity.

The chemical nature of this chain can be varied. We shall compare in this report two similar models including an aliphatic chain linked to the meso phenyl groups either through ether (compound A, Figure 1) or through amide (compound B, Figure 2) bonds. The synthesis and the iron insertion and reduction of these compounds have been described elsewhere.³

The proton NMR spectra of the oxygen and carbon monoxide complexes of compound A are presented in Figure 1. Both are characteristic of diamagnetic complexes in which the pyrrolic proton resonances exhibit an AB type pattern due to the C_{2v} symmetry of the molecule, with symmetry planes passing through the methene bridges of the porphyrin ring. The large high-field shift of the resonance of the pyridine protons $H_{b,b'}$ is due to the ring current effect of the porphyrin¹² on the coordinated base, as observed in the zinc complex. In both complexes the pyrrolic protons remain, however, quasi-equivalent, but their resonances are shifted to high field by 0.4 ppm in the oxygen complex as compared to the carbon monoxide complex, indicating a larger electronic perturbation of the porphyrin ring in the former case.

The oxygen complex of compound B still exhibits an effective C_{2v} symmetry (Figure 2), but the pyrrole proton resonances are no longer quasi-equivalent ($\Delta\delta = 0.45$). Replacing O_2 by CO restores the quasi-equivalence at 8.6 and 8.7 ppm with a mean low field shift of about 0.5 ppm, as observed in compound A.

The large inequivalence of the pyrrolic protons indicates a preferential orientation of the oxygen molecule toward two opposite methene bridges, the observed C_{2v} symmetry resulting from a fast exchange between these two equivalent positions. In contrast, the quasi-equivalence of the pyrrole proton resonances in the oxygen complex of compound A should result from a fast exchange of the oxygen molecule between four quasi-equivalent similar orientations. The two directions defined by the two planes passing through opposite methene bridges are indeed nearly equivalent in the absence of large anisotropic effects introduced by the coordination of the pyridine residue. This is suggested by the symmetry observed for the carbon monoxide complexes, in which the ligand may be assumed to be axially oriented.¹³

There is a more direct evidence for the interaction of the oxygen molecule with the amide groups of the "distal" chain in compound B. The amidic protons are easily assigned by deuterium exchange during reduction in the presence of heavy water instead of light water (Figure 2). The corresponding resonances form two groups of two equivalent protons corresponding to the "distal" and "proximal" chains, respectively. They appear in the carbon monoxide complex at 6.7 and 6.9 ppm, at positions comparable to those in the zinc complex (6.6 and 6.7 ppm). In the oxygenated complex the resonance of one set of amide protons is shifted by

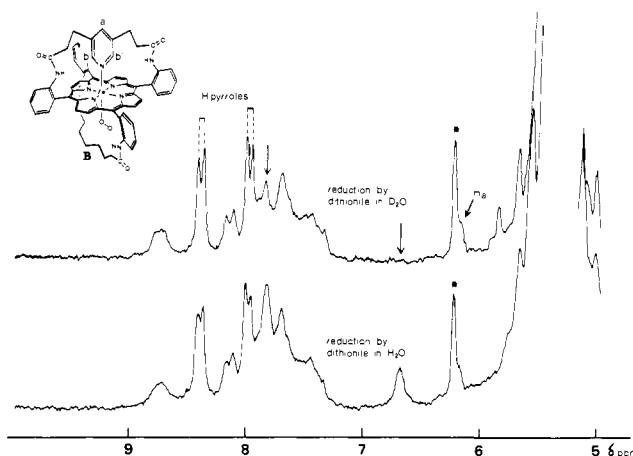


Figure 2. Low-field part of the proton NMR spectra of the oxygen complex of compound B in deuterated methylene chloride (from CEA, France) solution at -27 °C. The arrows denote the position of the resonances of the amidic protons assigned by deuterium exchange. The peak marked by an asterisk corresponds to the ^{13}C satellite of nondeuterated solvent impurity.

more than 1 ppm to low field and could be therefore assigned to the "distal" chain. This resonance should appear at an average position due to the fast exchange of the oxygen molecule between opposite directions. The intrinsic shift induced by the presence of the oxygen molecule for these protons is thus larger than 2 ppm. The preferential orientation of the oxygen molecule could result from dipole-dipole interaction or from a hydrogen-bond formation with the terminal oxygen atom. The magnitude of the low-field shift of the amide protons resonance strongly suggests direct bonding. The conformation of compound B permits this bonding. The bridged chain pulls the amidic protons toward the center of the porphyrin as shown by the high-field shift (up to 3 ppm) of the corresponding resonances in the zinc(II) or in the carbon monoxide iron(II) complexes relative to aromatic amides. Ring current shift calculations¹² allow one to estimate the position of the amidic protons and hence of the nitrogen atoms. The distance between one of the amide nitrogen atom and the terminal oxygen atom in a bent configuration may then be close to 3 Å, consistent with an intramolecular hydrogen bond. Crystallographic data for the picket-fence porphyrin model,⁹⁻¹¹ which bears similar amidophenyl groups, provide a larger distance of c.a. 4 Å, but the pivaloyl pickets are very flexible¹⁰ and not forced toward the center of the heme.

Modifications of the nature and stereochemistry (length and constraints in the carrying chain) of the axial base have already been introduced. These effects on the oxygen affinity and the magnetic properties are presently under investigation. The replacement of the pyridine base by an imidazole group in compound B adds 0.8 kcal mol⁻¹ (at 20 °C) to the free energy of binding for molecular oxygen to the 1.3 kcal mol⁻¹ already gained by introduction of the amide groups.³ The affinity of the complexes for oxygen is then comparable to that of the natural carriers^{14,15} but a meaningful interpretation of the thermodynamic and kinetic data still requires the separate measurements of enthalpic and entropic contributions.

Acknowledgment. This work was supported by the Institut National de la Santé et de la Recherche Médicale (Grant CRL No. 80 30 12).

Registry No. O_2 , 7782-44-7; CO, 630-08-0; O_2 -compound A, 82498-70-2; CO-compound A, 86323-19-5; O_2 -compound B, 82498-69-9; CO-compound B, 86323-20-8.

(12) Abraham, R. J.; Bedford, G. R.; Mc Neillie, D.; Wright, B. *Org. Magn. Reson.* 1980, 14, 418-425.

(13) Peng, S. M.; Ibers, J. A. *J. Am. Chem. Soc.* 1976, 98, 8032-8036.

(14) Imai, K.; Yonetani, T.; Ikeda-Saito, M. *J. Mol. Biol.* 1977, 109, 83-97.

(15) Wang, M. Y. R.; Hoffman, B. M.; Shire, S. J.; Gurd, F. R. N. *J. Am. Chem. Soc.* 1979, 101, 7394-7397.